

A Plausible Galactic Spiral Pattern and its Rotation Speed

M. Martos¹, X. Hernandez¹, M. Yáñez¹, E. Moreno¹, and B. Pichardo²

¹ *Instituto de Astronomía, Universidad Nacional Autónoma de México A. P. 70–264, México 04510 D.F., México*

² *University of Wisconsin, Department of Astronomy 475 N. Charter St. Madison, WI 53706, U.S.A.*

6 December 2018

ABSTRACT

We report calculations of the stellar and gaseous response to a Milky Way mass distribution model including a spiral pattern with a locus as traced by K-band observations, over imposed on the axisymmetric components in the plane of the disk. The stellar study extends calculations from previous work concerning the self-consistency of the pattern. The stellar response to the imposed spiral mass is studied via computations of the central family of periodic and nearby orbits as a function of the pattern rotation speed, Ω_p , among other parameters. A fine grid of values of Ω_p was explored ranging from 12 to 25 $km\ s^{-1}\ kpc^{-1}$. Dynamical self-consistency is highly sensitive to Ω_p , with the best fit appearing at 20 $km\ s^{-1}\ kpc^{-1}$. We give an account of recent independent pieces of theoretical and observational work that are dependent on the value of Ω_p , all of which are consistent with the value found here; the recent star formation history of the Milky Way, local inferences of cosmic ray flux variations and Galactic abundance patterns. The gaseous response, which is also a function of Ω_p , was calculated via 2D hydrodynamic simulations with the ZEUS code. For $\Omega_p = 20\ km\ s^{-1}\ kpc^{-1}$, the response to a two-armed pattern is a structured pattern of 4 arms, with bifurcations along the arms and interarm features. The pattern resembles qualitatively the optical arms observed in our Galaxy and other galaxies. The complex gaseous pattern appears to be linked to resonances in stellar orbits. Among these, the 4:1 resonance plays an important role, as it determines the extent of the stellar spiral pattern in the self-consistency study here presented. Our findings seemingly confirm predictions by Drimmel and Spergel (2001), based on K band data.

Key words: Galaxy: kinematics and dynamics – Galaxy: spiral – Galaxy: fundamental parameters – Galaxy: structure – ISM: structure

1 INTRODUCTION

The comparison of near-infrared and optical images of external galaxies reveals interesting differences. Striking examples are M81 and NGC 2997 (see pictures in Elmegreen, D., 1981; and Block et al 1994, respectively). It is common to observe a smooth, simple 2-armed K band pattern but a more complex pattern in the optical blue band, often suggesting more arms and bifurcations (segments of arms that appear to be connected to a K band arm but are not detectable in the infrared). A two-armed smooth structure underlying a more complex morphology also appeared in the work of Grosbøl, Pompei and Patsis (2002): in a K band study of 53 nearby spirals, most galaxies displayed a grand-design, two-armed, symmetric pattern in their inner regions which often breakups into tighter winded, multiple arms further out. Nonlinear effects were invoked to explain such morphology.

In recent work, data from COBE-DIRBE have shed light into the Milky Way spiral pattern. Drimmel (2000), and Drimmel & Spergel (2001) have presented a comprehensive picture of how this pattern is like, presenting emission profiles of the Galactic plane in the K band and at 240 μm . The former data set, which suffers little absorption and traces density variation in the old stellar population, is dominated by a two-armed structure with a minimum pitch angle of 15.5°. At 240 μm , the pattern is consistent with the standard four-armed model, that corresponding to the distribution of the youngest stellar populations delineated by HII regions.

The conventional picture of the spiral pattern of our Galaxy maps at least 4 arms, named Norma, Crux-Scutum, Carina-Sagittarius and Perseus (for a recent review see Vallée 2002, who also reports a likely pitch angle of 12° for this pattern). Additionally, features such as the Orion spur at the Solar neighborhood have been revealed (Georgelin &

Georgelin 1976). Drimmel (2000) laid down, from the comparison, the hypothesis that the 4-armed structure is the gas response to the 2-armed “stellar” pattern.

Assuming that indeed the K band data is by far a better tracer of mass than the optical data of spiral structure, in this work we model the spiral pattern from the locus and pitch angle of Drimmel (2000) and study its self-consistency, a requirement we consider it must satisfy. As the answer strongly depends on the pattern speed, this study should yield a value for this fundamental Galactic parameter.

The value of the pattern speed of the Galaxy has been a matter of controversy for a long time. From the values proposed by Lin, Yuan & Shu (1969) of $\Omega_p = 11 - 13 \text{ km s}^{-1} \text{ kpc}^{-1}$, numbers in the range of 10-60 $\text{km s}^{-1} \text{ kpc}^{-1}$ have been used in the literature. In a previous paper (Pichardo et al 2003, hereafter P1), we explored the stellar dynamics in a full axisymmetric model for our Galaxy superimposing our modeling of mass distribution for the spiral pattern: the locus of Drimmel (2000), the optical locus of Vallée (2002), and a superposition of both. P1 did not assume the usual simple perturbing term (a cosine term for the potential) that had been used in the literature in the modeling of spiral arms: it is precisely the very prominent spiral structure in red light what suggests to us that such structure should be considered an important galactic component worthy of a modeling effort beyond the simple perturbing term. P1 modeling consists of a superposition of oblate spheroids for the spiral. Two different values of $\Omega_p = 15, 20 \text{ km s}^{-1} \text{ kpc}^{-1}$, were tried. The best self-consistency was achieved with $\Omega_p = 20 \text{ km s}^{-1} \text{ kpc}^{-1}$ for the locus and pitch angle of Drimmel (2000). Figure 7 of P1, a mosaic of our self-consistency test – explained below – for parameters including the global spiral mass and loci, exhibits a remarkably good response for this case which rules out the other 3 cases in the panel. In fact, the behavior at $\Omega_p = 20 \text{ km s}^{-1} \text{ kpc}^{-1}$ is so good that one can hardly envision an improvement on general theoretical grounds. The question that comes to mind is, given the spiral locus and pitch angle of Drimmel (2000), our adopted mass distribution modeling, and the spiral mass implied by observations of external galaxies applied to those parameters, now fixed, are there other values of Ω_p which also satisfy our self-consistency criterion to that accuracy? In this paper, we extend the self-consistency calculations to a finer range of values of Ω_p in order to answer that question. Once the best value is found, we put it to the test in two ways: calculating the gaseous response to find out whether it is consistent with the observed optical Galactic spiral pattern, which amounts to a test of Drimmel’s hypothesis. Finally, we review recent work using independent data sets which are sensitive to the value of Ω_p . This is another way of testing our prediction against “nature”, and not only versus different modeling approaches, as the subjects of those independent studies are quite different from our Galactic modeling effort.

A continued line of work by Contopoulos and collaborators (see, v.g. Patsis, Grosbøl and Hiotelis 1997 and references therein) has provided the framework to study the response of gaseous disks to spiral perturbations. In that paper, a comparison between SPH models with Population I features observed on B images of normal, grand design galaxies, showed that the 4:1 resonance generates a bifurcation of the arms and interarm features. Furthermore, Contopoulos

& Grosbøl (1986,1988) had shown that the central family of periodic orbits do not support a spiral pattern beyond the position of the 4:1 resonance, which thus determines the extent of the pattern. Weak spirals can extend their pattern up to corotation, from linear theory. A phenomenological link between resonances, the angular speed, and the stellar and gas patterns in spirals is complemented by the study of Grosbøl and Patsis (2001) using deep K band surface photometry to analyze spiral structure in 12 galaxies. They find that the radial extent of the two-armed pattern is consistent with the location of the major resonances: the inner Lindblad resonance (ILR), the 4:1 resonance, corotation and the outer Lindblad resonance (OLR). For galaxies with a bar perturbation, the extent of the main spiral was better fitted assuming it is limited by corotation and the OLR. Using $H_0 = 75 \text{ km s}^{-1} \text{ Mpc}^{-1}$, the pattern speed was found to be for the entire sample of the order of $20 \text{ km s}^{-1} \text{ kpc}^{-1}$, and remarkably, not a sensitive function of morphological type or total mass.

In the following section we describe our results for the stellar orbital response to the imposed spiral pattern, through which Ω_p is determined.

2 ORBITAL SELF-CONSISTENCY MODELING, INFERRING Ω_P

As in P1 our axisymmetric Galactic model is that of Allen & Santillán (1991), which includes a bulge and a flattened disk proposed by Miyamoto & Nagai (1975), together with a massive spherical dark halo. We coupled to this mass distribution a spiral pattern modeled as a superposition of inhomogeneous oblate spheroids along a locus that fits the K band data of Drimmel (2000), with a pitch angle of 15.5° . P1 describes in detail the parameters of the spheroids, which briefly are: the minor axis of the spheroids is perpendicular to the Galactic plane and its length is 0.5 kpc; the major semi-axes have a length of 1 kpc. Each spheroid has a similar mass distribution. Different density laws, linear and exponential, were analyzed, finding no important differences.

The total mass in the spiral is fixed such that the local ratio of spiral to background (disk) force have a prescribed value. Seeking sensible values for this ratio, we used the empirical result of Patsis, Contopoulos and Grosbøl (1991), where self-consistent models for 12 normal spiral galaxies are presented, a sample including Sa, Sb and Sc galaxies. Their Figure 15 shows a correlation between the pitch angle of the spiral arms and the relative radial force perturbation. The forcing, proportional to the pitch angle, is increasing from Sa to Sc types in a linear fashion. For our pitch angle of 15.5° , the required ratio for self-consistency is between 5% and 10%. As shown in P1, the ratio is a function of galactocentric distance R. The authors consider strong spirals those in which the ratio is 6% or more.

We found that, in order to obtain relative force perturbations in the 5% to 10% range, our model requires a mass in the spiral pattern of $0.0175 M_D$, where M_D is the mass of the disk. With that choice, our model predicts a peak relative force of 6%, and an average value, over R, of 3%. Other spiral masses were explored, but the analysis favours this case, borderline but on the weak side of the limit separating linear (weak) and non-linear (strong) regimes considered

by Contopoulos & Grosbøl (1986, 1988). It is worth noticing that previous results were obtained using rather simplified galactic models, in which the relative amplitude of the spiral perturbation was taken as a fixed few percent of the axisymmetric force at all radii. To illustrate a reference value, Yuan (1969) proposed 5%.

We follow the technique of Contopoulos & Grosbøl (1986) to compute the ratio of the average density response and the imposed density, $\rho_r/\rho_i(R)$, calculating a series of central periodic orbits and using flux conservation between every two successive orbits. A dynamically self-consistent model will be one in which $\rho_r/\rho_i(R)$ does not deviate significantly from unity at any R; it will be a potential in which the orbits of stars will produce density enhancements in phase with the imposed pattern. Hence, $\rho_r/\rho_i(R)$ is a merit function for the dynamical self-consistency of the proposed spiral pattern. We then sample the unknown parameter Ω_p throughout a fine grid of values, and determine its optimal value as the one for which $\rho_r/\rho_i(R)$ is as flat and as close to unity as possible over the range R: [3.3, 12] kpc. This yields $\Omega_p = 20 \text{ km s}^{-1} \text{ kpc}^{-1}$ as a prediction of our analysis. The response is quite sensitive to Ω_p : nearby values such as 19 or 21 $\text{km s}^{-1} \text{ kpc}^{-1}$ showed noticeable differences. The range explored spanned values from 12 to 25 $\text{km s}^{-1} \text{ kpc}^{-1}$.

In Figure 1 we show the results for the case $\Omega_p = 20 \text{ km s}^{-1} \text{ kpc}^{-1}$. On the Galactic plane, the assumed spiral pattern and a set of stellar periodic orbits are drawn, with response density maxima shown by black squares. Notice the close coincidence of these with the locus of the imposed pattern within the boxy-like orbit which marks the 4:1 resonance. In the old kinematic-wave interpretation of orbital support for the spiral, one can see support inside the resonance, and an abrupt change corresponding to an off-phase response to the spiral outside it. Also dependent on Ω_p is the fact here displayed that the pattern would be dynamically terminated at the position of the 4:1 resonance (here at R = 7 kpc), as predicted by Contopoulos and collaborators.

3 CALCULATING THE GASEOUS RESPONSE TO THE BEST FIT POTENTIAL

Having determined shape, number of arms and total mass content of the spiral pattern from observations, and having inferred the optimal Ω_p from dynamical self-consistency, we now study the response of the gaseous disk to such a spiral potential through hydrodynamical simulations.

Figure 2 shows the gas response to the imposed pattern with $\Omega_p = 20 \text{ km s}^{-1} \text{ kpc}^{-1}$. The locus is indicated with open squares. We performed 2D numerical simulations in polar coordinates using the ZEUS code (Stone & Norman, 1992, a,b), without including gas self gravity. The numerical grid covers 2π radians and a radial range from 1 to 15 Kpc; however, we disregard results internal to R = 3.3 kpc, due to the influence of boundary conditions (b.c.). The calculation is made in the rotating spiral pattern frame of reference. Resolution is 500x500 zones and the b. c. are inflow-outflow (inner to outer) in R and periodic in the azimuth ϕ . The temperature was fixed at 8000 K, and the simulation is isothermal given the short cooling timescales compared to the dynamical timescales. The disk reaches a nearly steady state rapidly, which was followed in this case for 3 Gyr. The

system is initialized with velocities from the Galactic model rotation curve, adding the spiral source terms through an input table for ZEUS, and an exponential gas density law with a radial scale length of 15 kpc and a local value of about 1.1 cm^{-3} (see Martos & Cox 1998).

In between the imposed two-armed pattern, another two-armed pattern emerges, which displays a sharp shock with a maximum strength along the spiral between, roughly, 5 and 7 kpc in R. At R around 5 kpc, the arm bifurcates, and the shock strength weakens near R = 7 kpc. This position is quite close to the 4:1 resonance. On each side, this new “optical” two-armed pattern ends up in a corotation island. In the figure, the Solar position is along a radial line from the Galactic center (the origin of both the inertial and the rotating frames) at 20° from the primed (rotating) \hat{x} axis (Freudenreich 1998). Following the “K band” pattern there is a slightly offset gaseous response to the imposed potential, making the gas response a four-armed pattern.

A number of caveats apply to our gas simulation: one is that the strength of the shocks will considerably diminish in a full 3D, MHD simulation (the inclusion of the vertical direction and magnetic field was considered in Martos & Cox 1998). Recent simulations in full, realistic Galactic models are scarce: Gómez & Cox (2002) employed the Galactic model of Dehnen and Binney (1998). However, their value of Ω_p (12 $\text{km s}^{-1} \text{ kpc}^{-1}$) places the 4:1 resonance beyond 22 kpc, far out from the observed pattern extent. For that Ω_p , bifurcations and much of the rich structure is removed and the pattern becomes ring-like (Yáñez & Martos 2004). Another important component not included yet in these simulations is the Galactic bar, which we recently modeled (Pichardo, Martos & Moreno 2004, hereafter P2). Englmaier & Gerhard (1999) studied the gas dynamics in the bar potential determined by data. Their value of Ω_p is 60 $\text{km s}^{-1} \text{ kpc}^{-1}$. This work reproduces many features of the inner Galaxy. There is then a large difference in the angular speeds of bar and spiral. The bar-spiral coupling was considered by Bissantz, Englmaier & Gerhard (2003) in a comprehensive study that assembles the available data sets and SPH simulations in gravitational potentials determined from the near-infrared luminosity of the bulge and disk, and in some cases, an outer halo and a spiral model for the disc. This work contains models allowing for different pattern speeds for bar and spiral. Their optimal values, at the same position of the bar corotation and bar orientation adopted here, are found to be 60 and 20 $\text{km s}^{-1} \text{ kpc}^{-1}$ for the bar and the spiral, respectively.

For the spiral pattern, Drimmel & Spergel (2001) find that the arm strength begins to fall off at about $.85R_{Sun}$. This is just too close to the R = 7 kpc position of the 4:1 resonance (for our determined Ω_p) to dismiss it as an accident. It seems to favor a scenario in which the details of the coupling bar-spiral are not crucial to the dynamics at radii greater than 7 kpc or so. P2 proposes three different models for the Galactic bar mass distribution: an inhomogeneous ellipsoid, a prolate spheroid, and a superposition of ellipsoids fitting the observed boxy isophotes. There are strong model-dependent kinematics near the bar. Follow up work indicates to us that, while there is a large dispersive effect on orbits inside or near the bar region, at the Solar position the effect is minor. For instance, bar-induced vertical dispersive motion occurs only inside R=4 kpc. However,

see Mühlbauer and Dehnen (2003), who conclude that at least the lowest order deviations from axisymmetric equilibrium in the local kinematics can be attributed to the bar. The comparison with the effects of the spiral structure is deferred to a future paper. We argue that the result obtained by Bissantz, Englmeier & Gerhard (2003), in a study incorporating dynamics of bar and spiral, is a strong support to our claim that, even without the presence of the bar in our model, our predicted value should provide a valid comparison to first order with independent studies relying on Ω_p at the Solar position and beyond.

4 RECENT INDEPENDENT DETERMINATIONS OF Ω_p

From the data in Figure 2 one can directly obtain the gas surface density along a circle with the radius of the Sun's orbit. In the most simplistic circular approximation (the orbit has radial excursions of the order of 2 kpc), there are two main peaks of similar densities, and several local maxima of lower density. The mass contrast is consistent with K-band observations (Kranz, Slyz & Rix 2001), who quote an arm/interarm density contrast for the old stellar population of 1.8 to 3 for a sample of spiral galaxies. Interestingly, these two peaks have surface densities in reasonable agreement with the expected threshold density for star formation, a value of approximately $10 M_\odot pc^{-2}$ (Kennicutt 1989), in which we are considering the reduction in the shock compression due to the magnetic field and 3D dynamical effects. Other local maxima are factors of 3 or more below that value, making any associated burst of star formation a less likely event.

With $\Omega_p = 20 km s^{-1} kpc^{-1}$, the time baseline in the rotating frame for a circular orbit of that radius is very approximately 1 Gyr at our assumed Solar radius. We found that the two density peaks mentioned above are separated in time by ≈ 0.5 Gyr. We expect then that periodicity for enhanced star formation. We note that if self gravity were included the density contrast would increase, making the predicted periodicity for star formation more evident.

It is interesting to compare this prediction with recent results of direct inferences of the star formation history of the solar vicinity. Hernandez, Valls-Gabaud and Gilmore (2000) analyze the colour-magnitude diagram of the solar neighbourhood as seen by the Hipparcos satellite, and using Bayesian analysis techniques derive the star formation history over the last 3 Gyr. These authors find an oscillatory component with a period of 0.5 ± 0.1 Gyr. By studying the age distribution of young globular clusters, de la Fuente Marcos & de la Fuente Marcos (2004) obtain a periodicity in the recent star formation history at the solar circle of 0.4 ± 0.1 Gyr. It is remarkable that two distinct and independent assessments of the recent star formation history at the solar circle yield a periodicity which is perfectly consistent with the density arm crossing period we derive in this study.

Shaviv (2002) finds that the cosmic ray flux reaching our Solar System should periodically increase with each crossing of a Galactic spiral arm. Along the same lines of last section, over a time baseline of the past 1 Gyr, we added our estimated magnetic field compression from Martos & Cox (1998) to plot the expected synchrotron flux variations mov-

ing along the Solar circle and assuming the mass distribution fixed in time. We find 6 local maxima with fluxes that are higher than today's flux. This is the same number of peaks satisfying that condition in Shaviv's work, who plots the ratio cosmic ray flux/today's cosmic ray flux obtained from a sample of 42 meteorites, which they relate to climate changes in Earth. Shaviv (2002) reports a period of 143 Myr for the episodes (crossings) from meteorites data, which leads to a value of $|\Omega_p - \Omega_{Sun}| \gtrsim 9.1 \pm 2.4 km s^{-1} kpc^{-1}$, which is marginally consistent with our preferred value.

Andrievsky et al. (2004) report on the spectroscopic investigation of 12 Cepheids situated at Galactic radii of 9 to 12 kpc, where they find an abrupt change in metallicity. The region 10 to 11 kpc appears to be the most important, and the change in metallicity is explained in terms of the assumed position of corotation. That position is precisely the location of corotation in our modeling, if the value $\Omega_p = 20 km s^{-1} kpc^{-1}$ is adopted. However, it is worth noticing that the assumed R_{Sun} is 7.9 kpc, 0.6 kpc less than the value for this fundamental parameter in our Galactic model. This difference might not alter their results for the change in metallicity level in the vicinity of corotation, given the large width of the density enhancement caused by the corotation islands at about $R = 11$ kpc in two extended regions of our Figure 2.

5 DISCUSSION

As found by Contopoulos & Grosbøl (1988), self-consistency is improved by introducing velocity dispersion; this is a realistic effect that can only be neglected by arguing that in strong spirals nonlinearity dominates. For our Galaxy, the observations of Drimmel & Spergel (2001) suggesting the termination of the spiral at the position of the 4:1 resonance indicate a marginally strong spiral in Contopoulos & Grosbøl's (1988) framework. On the opposite side, our best self-consistent model is found at the lowest spiral mass considered in P1, $0.0175 M_D$, for which no stochastic motion was found. From this fact, a weak spiral and a linear regime come to mind. A possible solution to this issue could be that, while the strength of the spiral begins to fall at the 4:1 resonance, termination occurs at corotation, as predicted for the weak case in that framework. However, the quite different modeling of the galactic – particularly, spiral – mass distribution used in their studies and ours could make an interpretation of our results in their framework an unfair one. At any rate, the response at our best Ω_p is so flat that there appears no need to invoke velocity dispersions. In an analysis based on periodic orbits, such as ours, such dispersion will be small. Other close values of Ω_p could be improved by this effect in a study out of the scope of this work, involving many orbits departing from the periodic ones and hence subjected to larger velocity dispersions.

We conclude that a two-armed density spiral imposed taking into account observational restrictions from K-dwarf distributions yields an optimal dynamically self-consistent model, for values close to $\Omega_p = 20 km s^{-1} kpc^{-1}$. The fact that various independent estimates of this quantity, sensitive to highly distinct physics, yield values for Ω_p in agreement with our estimation, gives us confidence in the result. In regard to the gaseous response, we notice that the indepen-

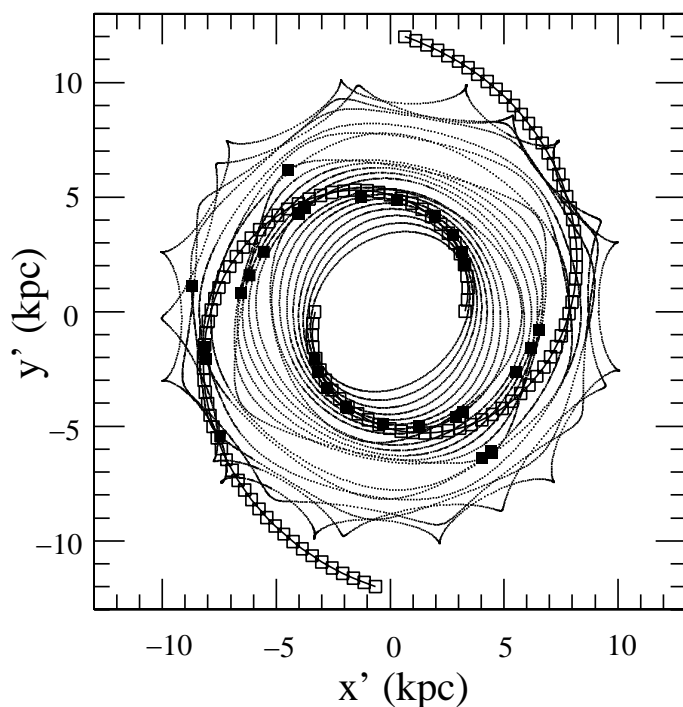


Figure 1. Self-consistency analysis for $\Omega_p = 20 \text{ km s}^{-1} \text{ kpc}^{-1}$. The proposed spiral locus is shown with open squares. A set of periodic orbits are traced with continuous lines, and the maxima in the response density are the filled (black) squares. The frame of reference is the rotating one where the spiral pattern is at rest

dent studies we quote for comparison are not only consistent with the value found here for Ω_p , but also with a density distribution corresponding to a 4-armed gaseous pattern with structural features reminiscent of optical observations of our Galaxy and other spirals.

6 ACKNOWLEDGMENTS

We thank an anonymous referee for helpful comments which significantly improved the clarity of the final presentation. E. Moreno, M. Martos, B. Pichardo, M. Yáñez acknowledge financial support from **CoNaCyT** grant 36566-E, and UNAM-DGAPA grant IN114001.

REFERENCES

- Allen, C. & Santillán, A., 1991, *RMxAA*, 22, 255
Andrievsky, S.M., Luck, R.E., Martin, P. & Lépine, J.R.D., 2004, *A & A* 413, 159
Bissantz, N., Englmaier, P., & Gerhard, O., 2003, *MNRAS*, 340, 949
Block, D.L., Bertin, G., Stockton, A., Grosbøl, P., Moorwood, A.F.M., Pletier, R.F. 1994, *A & A*, 288, 365
Contopoulos, G. & Grosbøl, P., 1986 *A & A*, 155, 11
Contopoulos, G. & Grosbøl, P., 1988 *A & A*, 197, 83
Dehnen, W. & Binney, J., 1998, *MNRAS*, 294, 429
Drimmel, R., 2000, *A & A* 358, L13
Drimmel, R., & Spergel, D. 2001, *ApJ* 556, 181
Elmegreen, D., 1981, *ApJ Suppl.*, 47, 229
Englmaier, P. & Gerhard, O., 1999, *MNRAS*, 304, 512
Freudenreich, H. T., 1998, *ApJ*, 492, 495

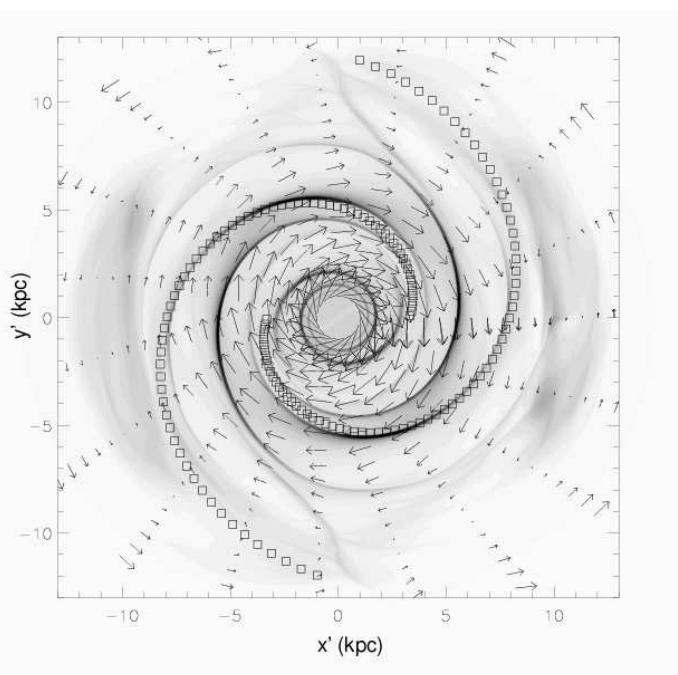


Figure 2. Simulation with the ZEUS code of the gas response to a spiral pattern with $\Omega_p = 20 \text{ km s}^{-1} \text{ kpc}^{-1}$, open squares, shown in the rotating frame of the spiral pattern after 2.55 Gyr of evolution. The arrows give the velocity field, their size being proportional to the speed, with the maximum speed shown being 212 km s^{-1} . Dense zones correspond to dark regions.

- de la Fuente Marcos, R., de la Fuente Marcos, C., 2004, *NewA*, 9, 475
Gómez, G. & Cox, D.P., 2002, *ApJ* 580, 235
Georgelin, Y.M. & Georgelin, Y.P., 1976, *A & A* 49, 57
Grosbøl, P. & Patsis, P., 2001, *ASP Conference Series* 230, 149
Grosbøl, P., Pompei, E. & Patsis, P., 2002, *ASP Conference Series* 275, 305
Hernandez, X., Valls-Gabaud, D. & Gilmore, G., 2000, *MNRAS* 316, 605
Kennicutt, R., 1989 *ApJ* 344, 685
Kranz, T., Slyz, A. & Rix, H.-W., 2001, *ApJ* 562, 164
Lin, C.C., Yuan, C. & Shu, F., 1969, *ApJ* 155, 721
Martos, M. & Cox, D.P., 1998, *ApJ*, 509, 703
Miyamoto, M. & Nagai, R., 1975, *Pub.Astr.Soc.Japan*, 27, 533
Mühlbauer, G. & Dehnen, W., 2003, *A & A*, 401, 975
Patsis, P.A., Contopoulos, G., & Grosbøl, P., 1991, *A & A*, 243, 373
Patsis, P.A., Grosbøl, P. & Hiotelis, N., 1997, *A & A* 323, 762
Pichardo, B., Martos, M., Moreno, E. & Espresate, J., 2003, *ApJ* 582, 230 (P1)
Pichardo, B., Martos, M. & Moreno, E., 2004, *ApJ*, accepted, astro-ph/0402340 (P2)
Shaviv, N.J., 2002, *Phys. Rev. Lett.* 89, 051102
Stone, J.M. & Norman, M.L., 1992a, *ApJS*, 80, 753
Stone, J.M. & Norman, M.L., 1992b, *ApJS*, 80, 791
Vallée, J.P., 2002, *ApJ* 566, 261
Yáñez, M. & Martos, M., 2004, in preparation
Yuan, C., 1969, *ApJ* 158, 871